Charging of Ellipsoidal Monomers

Kevin Bombardier

***Abstract*—Modeling the charging and aggregation of monomers in dust aggregates in a plasma helps in understanding processes such as planetary formation. Many dust charging models assume the monomers to be spherical. However, there is evidence to suggest that dust in some astrophysical environments is not exactly spherical; a better approximation would be to model ellipsoidal monomers. In many astrophysical environments, grains are also charged from collections of plasma species or radiation. This paper discusses an algorithm used to calculate the charge on ellipsoidal monomers and compare the results to spherical monomers. Using a modified version of orbital motion-limited (OML) theory, the current density to the surface of a grain can be computed to approximate the charge on a given monomer. The current to each monomer's surface is calculated using a line of sight (LOS) approximation. The LOS approximation assumes that only the paths from a given point on a monomer that are not blocked by another monomer contribute to the charging of that monomer. This current is then used to calculate the charge and dipole moment. The charge and dipole moment on an ellipsoidal monomer can be compared to that of a spherical monomer to better understand the coagulation process.**

***Index Terms*—Dust coagulation, ellipsoidal monomers, planetestimal formation, charging.**

I. Introduction

THE coagulation of dust grains is an important area of research in several fields, especially in the study of planetesimal formation where dust coagulation is thought to be the first step in planetary formation [1]. When immersed in a plasma or radioactive environment, these dust grains acquire a charge that influences the formation of dust aggregates. Thus, it is crucial to be able to understand the charge on these aggregates to better understand planetary formation.

Numerous studies have modeled the dust grains as spherical monomers [2],[3]. However, the dust grains are not always spherical. Previous research has shown differences in aggregate morphology [4]. However, these models only considered ballistic collisions between mutual grains. As noted above, grains in astrophysical environments can be charged. The case of calculating the charge on these ellipsoids is a much more difficult task due to the loss of spherical symmetry [2]. By modeling dust grains to be ellipsoidal, the impact that the charge has on dust coagulation can be better understood through careful study. Having modeled the charging process of ellipsoidal monomers, it is possible to compare the charging of spherical monomers to that of ellipsoidal monomers. The charge influences the interaction between dust monomers, and this results in a different overall structure (or fractal dimension) for dust aggregates [2].

The charge distribution and the dipole moment on a single monomer are also of interest. For a single spherical monomer, the charge distribution is symmetric around the monomer. There is no net dipole for a single spherical monomer. This differs from an ellipsoidal monomer's charge distribution and dipole moment. This piece of information is of particular importance because a dipole moment would affect the overall evolution of an aggregate.

This paper discusses a modified version of OML_LOS code for the charging of dust aggregates which assumes that each monomer to be ellipsoidal rather than spherical. Results for the charge, charge distribution, and the dipole moment for an ellipsoidal monomer is also discussed.

II. Method

The code used to model the charging of dust particles is based on the OML_LOS code described in [2],[3]. Modifications were made to the code to take into account ellipsoidal geometry. The algorithm calculates the charge of the monomers using a modified orbital motion limited (OML) theory with a line of sight (LOS) approximation.

A. Modified OML Theory

In orbital motion limited theory, the current density to any given point on monomer α is given by

$$J = n_{\alpha\infty} q_\alpha \int f v \cos\eta \, d^3\vec{v} \qquad (1)$$

where $n_{\alpha\infty}$ is the number density of plasma species α far away from a monomer's potential well, q_α is the charge of the plasma species, f is the distribution function, η is the angle between the velocity vector and the surface normal vector, and this integral is over the velocity space $d^3\vec{v}$ that does not include "blocked" orbits [2]. The distribution function is assumed to be Maxwellian and is given by

Manuscript received August 2011. This work was supported in part by the National Science Foundation under the Research Experience for Undergraduates program.

Kevin Bombardier did research with Baylor University (e-mail: SR_Kevin_Bombardier@baylor.edu)

Lorin S. Matthews is with the Physics department at Baylor University, Waco, TX 76798 (email: Lorin_Matthews@baylor.edu).

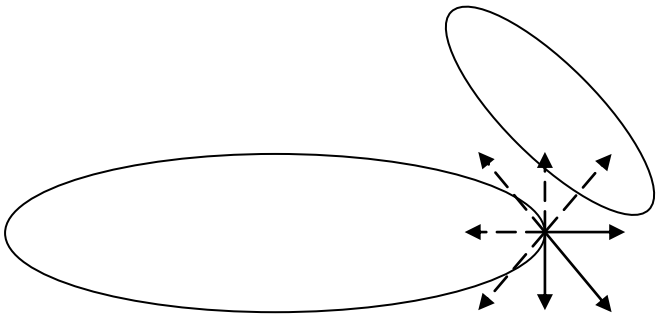

Fig. 1. The lines illustrate the lines of sight for a patch on a monomer. Dashed lines indicated blocked lines of sight.

$$f = \left(\frac{m_\alpha}{2\pi k T_\alpha}\right)^{\frac{3}{2}} \exp\left(-\frac{m_\alpha}{2kT_\alpha}v^2 - \frac{q_\alpha \phi}{kT_\alpha}\right) \quad (2)$$

where T_α is the temperature of the plasma species, m_α is the mass of the plasma species, k is the Boltzmann's constant, and ϕ is the dust grain's potential [2].

B. Line of Sight Approximation

By making the substitution

$$d^3\vec{v} = v^2 dv d^2\Omega \quad (3)$$

the integral over speed and direction can be separated where $d^2\Omega$ is the differential solid angle of orbits that are not blocked [2]. Any incoming charged particles are assumed to move in a straight line. The solid angle of integration is found by defining $m \times n$ test directions, where m is the number of angles of elevation θ and n is the number of azimuthal angles, ϕ. Any blocked lines of sight, as shown in Figure 1, are removed from the solid angle in the integration.

C. Code modifications

The code was modified to calculate the charge and dipole moment for ellipsoidal monomers rather than spherical ones. Test points were used to determine which lines of sight to remove from the integration. The test points were defined by points on a unit sphere of a 21 by 20 matrix created by assigning a range in theta (which denoted the azimuth angle) and a range in phi (which denoted the elevation angle) to use as lines of sight and to make ellipsoids out of the unit spheres. These points were used to determine which lines of sight to remove from the integration. Also, the points were used to divide the surface of the ellipsoid into patches.

One difference from the original code was in finding the cosine of the angles between incoming lines of sight and the unit normal vectors for a surface patch. In a spherical monomer, one is able to find the cosine of the angle between each LOS and the unit normal vector rather easily. This is because the unit normal vector for a point on a unit sphere is the vector pointing from the center to the point itself. Since the vector to a point on a sphere is also its normal vector, the dot product of each vector direction can be computed to find all possible cosine factors. However, for an ellipsoid, this is not as simple. The approach used to generalize this section of the code instead calculated the gradient of the equation for an ellipsoidal given by

$$x^2 / a^2 + y^2 / b^2 + z^2 / c^2 = 1, \quad (4)$$

where a, b, and c are the lengths of the semi-axes of the x, y, and z coordinates respectively. The gradient, calculated at the center of each patch, is the normal vector of the ellipsoid, so once this vector is normalized, the cosine of the angles that the unit normal vectors and the lines of sight makes with each other can be calculated.

Another major change to the code was in calculating the surface area of patches on the ellipsoids. For a sphere, it is relatively simple to arrange the test points such that the surface area on each patch of the sphere is constant. However, on an ellipsoid, this is not so simple (if even possible). Instead, the surface area of each patch was calculated individually. It is important to note that the modified version of the code used a numerical integration to find the surface area of these patches. The surface area is given by

$$SA = \int_{\phi_{\min}}^{\phi_{\max}} \sin\phi \int_{\theta_{\min}}^{\theta_{\max}} \sqrt{a^2 b^2 \cos^2\phi + c^2\left(b^2\cos^2\theta + a^2\sin^2\theta\right)\sin^2\phi}\, d\theta\, d\phi \quad (5)$$

where θ is the azimuth angle, ϕ is the polar angle, and a,b,c are the lengths of the x,y,z semi-axes respectively [6]. It should be noted that the surface area of the patches near the poles is small and not as accurate as the other patches (where the elevation is $\pm \pi/2$). However, since these patches are small compared to the other patches, the overall charge is hardly affected.

The last main change to the code was in calculating the LOS factor. The LOS factor was used to calculate the charge and is part of the LOS approximation discussed earlier. To find the LOS factor, the free lines of sights were determined which indicated which points on the ellipsoid were blocked and which were open. The LOS factor is

$$LOS\_factor = \int \cos\eta\, d\Omega \quad (5)$$

where η and $d\Omega$ are the same as mentioned earlier [5]. The calculation to approximate the LOS factor is

$$LOS\_factor =$$

$$\sum_m \sum_i \cos\eta_{mi} \times SA_{mi} \times free\_LOS_{mi} \qquad (6)$$

where m and i are indices indicating the azimuth and elevation of a point.

The code was modified to change its approach on how to determine if a given point on a monomer was inside another monomer or not. In the case of spheres, the symmetry of the sphere makes this task simpler because the radius of a sphere is constant. The original OML_LOS code calculated the distance from every point on each monomer to the center of each monomer. If the distance from a point on a monomer to the center of another monomer was less than the radius of the other monomer, then that point was inside another monomer. The LOS would then be completely blocked. The modification first calculated the distances from the surface points on each ellipsoidal monomer to the center of each monomer. Once this was accomplished, these vectors were converted into each monomer's coordinate system. These vectors coordinates were plugged into

$$x^2 / a^2 + y^2 / b^2 + z^2 / c^2 \leq 1, \qquad (7)$$

where a,b,c were the lengths of the x,y,z semi axes respectively. If the above condition was satisfied (excluding the monomer where the point is located on), then that surface point would be inside (or on) another monomer; thus, its LOS would be completely blocked.

The code estimated which lines of sight were blocked by the monomer itself. For spheres, the curvature around any given point is the same. The curvature of a sphere allows for any angle that is "behind" the tangent plane for a given point on a sphere to be considered blocked in the integration. For ellipsoids, this is not exactly the case. However, computing the angles to eliminate is a much more difficult task. Instead, the same approach for spheres was used in the code. This approximation works well for ellipsoids that do not vary greatly from spheres. It is important to note that ellipsoids having a long semi-axis compared to its two other semi-axes will be less accurately modeled using this approach. A better approach might be to estimate the curvature by nearby points on the ellipsoid and to find the angles from there.

The last modification was in calculating blocked lines of sight due to other monomers blocking incoming charged particles. The code for ellipsoids took each LOS and converted them to each monomer's coordinate system (the origin at the center of the monomer). The lines were then parameterized in every monomer's coordinate system. The x,y,z components of the parameterized lines were used in equation (4). This forms a quadratic equation from the parametric variable. If the solutions were real, then there exists some point on the line that intersects the ellipsoid. Hence, that LOS would be blocked. If the solutions were imaginary, the LOS would be open (see Fig. 2).

D. Charging Conditions

The charge was calculated for a single monomer assuming that the electron and ion temperature were $T_e = T_i =$ 4637 K, as used in past simulations. The plasma number density was set at $n_{\alpha\infty}$ = 5 x 10^8 m^{-3} [2]. Both spheres and ellipsoids were charged and the results compared.

III. Results

The code calculated the case of spherical monomers first as to test whether the code worked properly. A spherical monomer of radius 3 x 10^{-6} m attained Q = 3.3540 x 10^{-16} C. This agrees with the previous version of OML_LOS for spheres which calculated Q = 3.3539 x 10^{-16} C. The charge distribution for a spherical monomer was plotted as shown in Fig. 3. For a sphere, the charge on a spherical monomer should be symmetric on any given monomer. The color of the surface patches indicates the patch charge divided by the surface area of the patch. The charge on the surface of a sphere is constant with some small variations at the poles. The variations are most likely due to the numerical integration of the surface area of the patches.

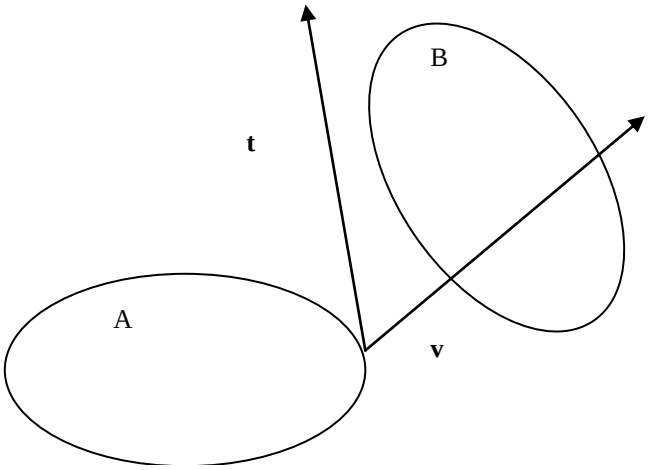

Fig 2. Vector **t** will yield imaginary solutions when its parametric equation is inserted into the equation for ellipsoid B and is an open LOS. The parameterization of vector **v** will yield real solutions and is a blocked LOS.

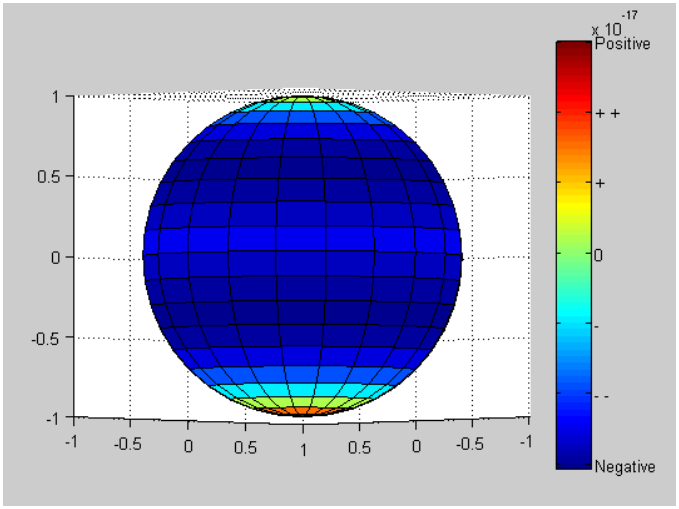

Fig. 3. The charge distribution on each patch on the sphere was plotted. Blue indicates a negative charge. Red indicates a positive charge. Overall the charge is symmetric except for some error at the poles as mentioned above.

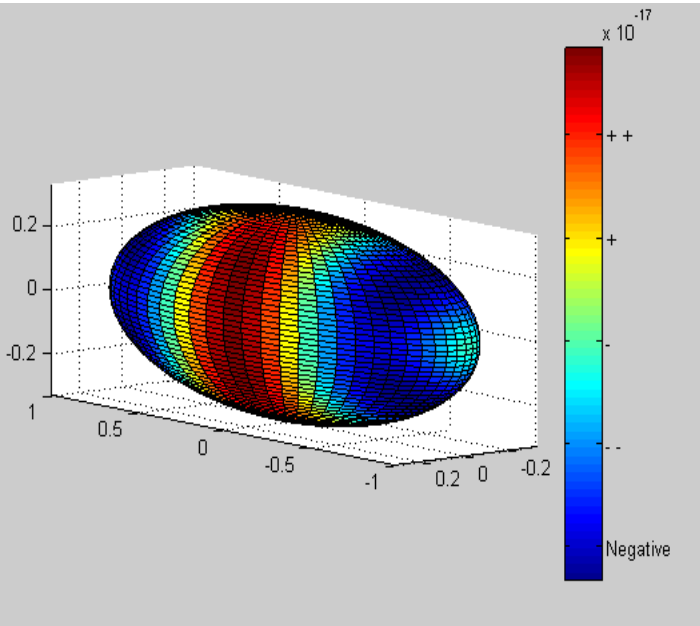

Fig. 4. Oblique view of the charge distribution on an ellipsoidal monomer. The colors represent the charge per surface area on each patch. More surface points were used to show the results more clearly.

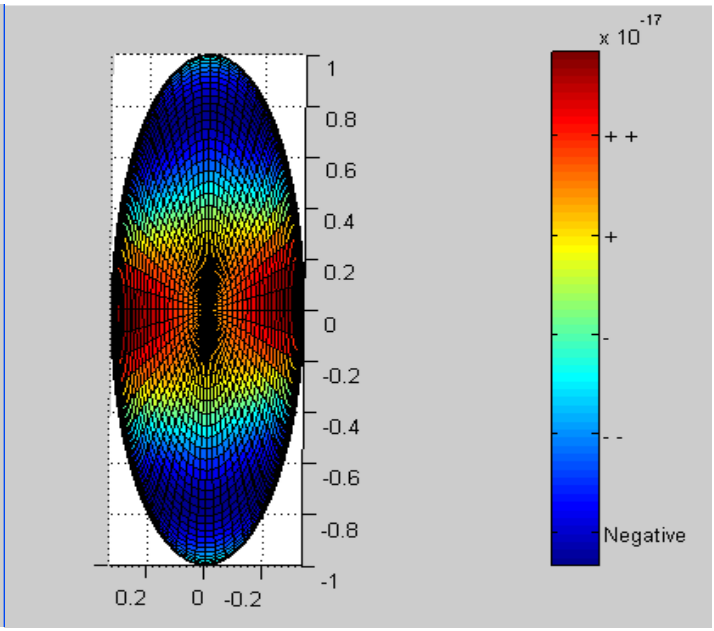

Fig. 5. Top view of the charge distribution on an ellipsoidal monomer. The colors represented are the same as in Fig. 3.

The charge on an ellipsoid with a = 3 × 10^{-6} m and a semi-axis ratio a:b:c = 1:1/3:1/3 was charged and obtained a charge Q = -1.75 x 10^{-16} C. This value is reasonable considering the surface area of this ellipsoid is smaller than the spherical monomer. The charge distribution on the ellipsoidal monomer is shown in Figs 4 and 5. The negative charge sits near the end of the semi-major axis for the ellipsoid. The positive charge sits near the semi-minor axes.

The dipole moment for this ellipsoid was also calculated in the code. This ellipsoid had a dipole moment vector of (1.0 x 10^{-22}) (-0.2300 , 0.0020, 0.0192) which indicates that the dipole points along the semi-major axis. The magnitude | p | ≈ 10^{-22} which is Qd, where d is the length of a semi-axis.

To further compare the results, a series of ellipsoids of constant volume and varying length/diameter ratios were charged and compared. The length is twice the semi-major axis length and the diameter is twice the semi-minor as used by Auer (See Fig. 6) [7]. The results were plotted to show the charge ratio versus the length/diameter ratio. The results were compared to the shape factor calculated by Auer et al [7] for varying ellipsoids using the computer program "Coulomb",

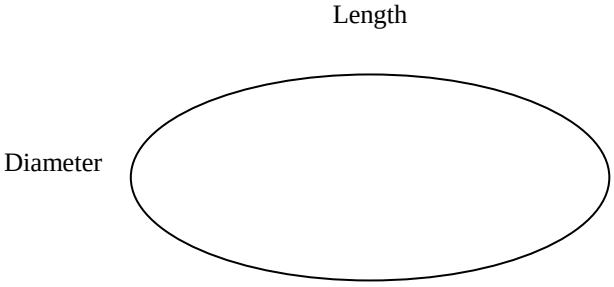

Fig. 6. The length is the semi-major axis of the ellipsoid and the diameter is the semi-minor axis of the ellipsoid.

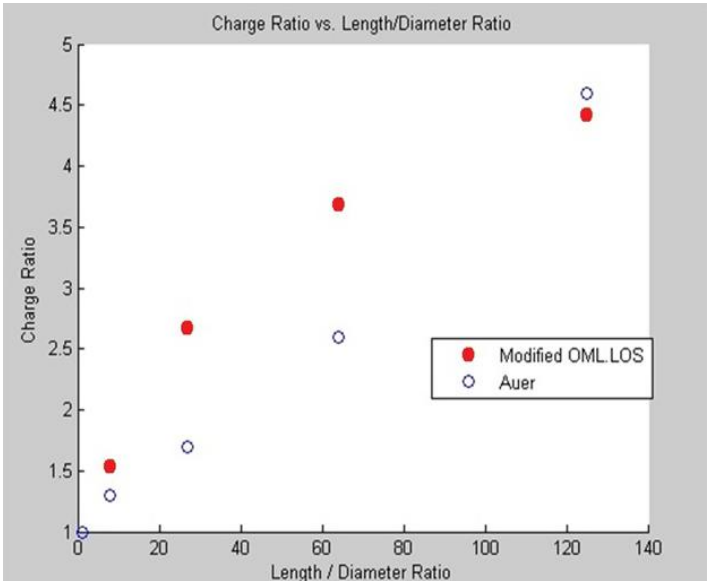

Fig. 7. The charge ratio versus the length/diameter ratio at a constant volume. T he charge increases as the length of the semi-major axis of the ellipsoid increases.

which solves Maxwell's equations in integral form. Ellipsoids of varying semi-axis length ratios at a constant volume were calculated using the modified OML_LOS code. Several projected data points from Auer et al were used in Fig. 7. In general, the modified OML_LOS code has a larger charge ratio than the data in [7]. This may be due to error introduced when ignoring the curvature of the ellipsoid.

IV. Conclusion

This model approximates the charge and dipole moment on ellipsoidal monomers. The charge on an ellipsoidal monomer is larger than that of a spherical monomer with the same volume. This indicates that the behavior of a

charged aggregate with ellipsoidal monomers would differ from a charged aggregate consisting of spherical monomers.

The charge distribution and the dipole moment on the ellipsoidal monomer are also of interest. There is a net dipole on the ellipsoidal monomer whereas the spherical monomer does not have one due to its symmetry. This may influence how charged ellipsoidal monomers prefer to collide in contrast to spherical ones. Ellipsoidal monomers will experience a torque due to this fact.

It should be noted that because of the approximation mentioned earlier in calculating which lines of sights are blocked by the monomer itself, the charges obtained may differ from their exact value. This approximation becomes less accurate as the magnitude of the ratio between the semi-major and the semi-minor axes increases.

V. Future Work

. By neglecting the curvature of the ellipsoid in determining what lines of sights are blocked by the monomer itself, an unwanted error is introduced into the model. Approximating the blocked lines of sight by the monomer itself more accurately would be preferred. A possible solution to this problem would be to estimate the curvature around a point by using nearby points to determine the blocked angles (See Fig. 8).

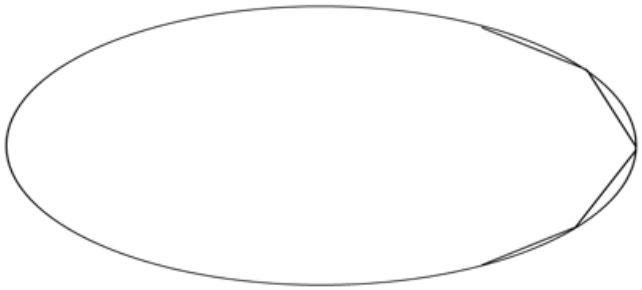

Fig. 8. A possible solution to better estimate the blocked lines of sight due to the monomer's own surface. Nearby points could be used to approximate the blocked angles.

This model will be applied by building charged aggregates from ellipsoidal monomers and compare the results to neutral aggregates as well as charged aggregates built from spherical monomers to better understand how charging affects an aggregate's evolution and shape.

Acknowledgment

I would like to thank Lorin S. Matthews and Jonathan Perry for all their help throughout this project. Thank you to everyone at CASPER who have been helpful throughout this experience. This work was funded by NSF grant PHY-1002637.

References

[1] L.S. Matthews, R.L. Hayes, M.S. Freed, and T.W. Hyde, "Formation of Cosmic Dust Bunnies," *IEEE Transactions on Plasma Science*, vol. 35, no. 2, pp. 260-264, Apr. 2007.

[2] L.S. Matthews and T.W. Hyde, "Charging and Growth of Fractal Dust Grains," *IEEE Transactions on Plasma Science*, vol. 36, no. 1, pp. 310-314, Feb. 2008.

[3] L .S. Matthews and T.W. Hyde, "Effect of dipole-dipole charge interactions on dust coagulation," *New J. Phys.* vol. 11, 2009.

[4] J.D. Perry, E. Gostomski, L.S. Matthews, and T.W. Hyde, "The Influence of Monomer Shape on Aggregate Morphologies," *Astronomy and Astrophysics*, 2011.

[5] M. Qianyu, L. Matthews, V. Land, and T.W. Hyde, " Charging of interstellar dust grains near the heliopause," Submitted to Astrophysical Journal, July, 2011.

[6] Weisstein, Eric W. "Ellipsoid." From MathWorld--A Wolfram Web Resource. http://mathworld.wolfram.com/Ellipsoid.html

[7] S. Auer, S. Kempf, and E. Grun, "Computed electric charges of grains with highly irregular shapes," *Workshop on Dust in Planetary Systems. pp. 177-180, Jan* 2007.